PROCEEDINGS OF SCIENCE

Finite density QCD from an effective lattice theory

Owe Philipsen[*1], **Jens Langelage**[2], **Stefano Lottini**[3], **Mathias Neuman**[1]
1*: Institute for Theoretical Physics, Goethe-University Frankfurt, 60438 Frankfurt, Germany*
E-mail: philipsen, neuman@th.physik.uni-frankfurt.de
2*: Institute for Theoretical Physics, ETH Zürich, CH-8093 Zürich, Switzerland*
ljens@phys.ethz.ch
3*: Neumann Institute for Computing at DESY, 15738 Zeuthen, Germany*
stefano.lottini@desy.de

We summarise recent attempts to describe finite density QCD by means of an analytically derived effective lattice theory formulated in terms of Polyakov loops. For sufficiently heavy quarks, the underlying strong coupling and hopping expansions are fully controlled and allow for continuum extrapolations of numerical results obtained in the effective theory. The sign problem of the latter can be cured by flux representations or the application of complex Langevin methods. We present the deconfinement transition and its critical endpoint as a function of pion masses and chemical potential. Simulations in the cold and dense regime are also possible, demonstrating the sudden transition to cold nuclear matter at zero temperature from QCD directly.

Xth Quark Confinement and the Hadron Spectrum
8-12 October 2012
TUM Campus Garching, Munich, Germany

[*]Speaker.

PoS(Confinement X)218

1. Introduction

QCD at finite baryon density remains a challenge for lattice simulations because direct Monte Carlo simulations are prohibited by the sign problem: the fermion determinant becomes complex for non-vanishing quark chemical potential μ and cannot be interpreted as part of a probability weight. Existing workarounds based on reweighting, Taylor expansions in μ/T or simulations at imaginary chemical potential followed by analytic continuation all introduce additional approximations which are valid for $\mu \lesssim T$ only, see [1]. The QCD phase diagram remains largely unkown and there are no QCD predictions for cold nuclear matter.

This motivates a new approach by analytically derived effective theories, which should simplify the computational problem while maintaining control over the systematic errors. An example is dimensional reduction at finite temperature [2], which relies on a sufficient scale separation $gT \ll \pi T$ between soft and hard modes in the thermal theory. The former then get integrated out perturbatively to produce a 3d effective theory for the soft modes, which can be readily simulated on the lattice. The approach is valid in the deconfined phase but fails to describe the deconfinement transition, since the perturbative step explicitly breaks the centre symmetry of Yang-Mills theory [3]. Alternative efforts write down the most general centre-symmetric 3d effective action for the soft modes [4] and fix the couplings by perturbative or even non-perturbative matching calculations [5]. However, for $SU(3)$ this remains a difficult task due to the high number of matching coefficients. In this contribution we summarise a recent solution to this problem by means of strong coupling expansions on the lattice. We describe how to derive a centre-symmetric 3d effective theory for thermal Yang-Mills theory and simulate it on the lattice. After successful completion of this step we include heavy quarks. The resulting theory still has a sign problem, but it can be overcome by applying flux representations [6] or a complex Langevin algorithm [7]. We compute the deconfinement transition as a function of quark mass and all chemical potentials. Finally, the cold and dense regime is also feasible and we obtain a clear signal for the onset of nuclear matter.

2. Yang-Mills theory

Starting point is the (3+1)-dimensional Wilson lattice action at finite temperature $T = (aN_\tau)^{-1}$,

$$Z = \int [dU_0][dU_i] \exp\left[\frac{\beta}{2N}\sum_p (\mathrm{Tr}U_p + \mathrm{Tr}U_p^\dagger)\right], \quad \beta = \frac{2N}{g^2}\,. \tag{2.1}$$

Finite temperature and the bosonic nature of the degrees of freedom imply the use of periodic boundary conditions in the time direction. Finer lattices correspond to larger N_τ for fixed physics. We now integrate out the spatial links in a strong coupling expansion and get schematically

$$Z = \int [dU_0] \exp[-S_{\rm eff}]\,; \tag{2.2}$$

$$-S_{\rm eff} = \ln \int [dU_i] \exp\left[\frac{\beta}{2N}\sum_p (\mathrm{Tr}U_p + \mathrm{Tr}U_p^\dagger)\right] \equiv \lambda_1 S_1 + \lambda_2 S_2 + \ldots \tag{2.3}$$

We expand about $\beta = 0$ and arrange the effective couplings $\lambda_n(\beta, N_\tau)$ in increasing order in β of their leading terms. Thus the λ_n become less important the higher n. The interaction terms S_n

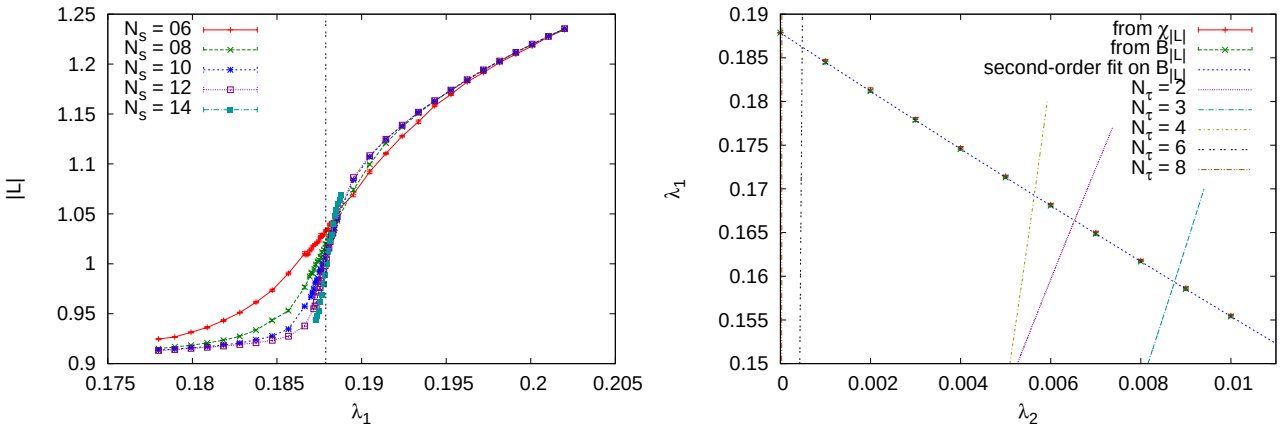

Figure 1: Left: Expectation value of $|L|$. With increasing spatial volume, a first order transition builds up, the infinite volume critical coupling is marked by a vertical line. Right: Critical line in the two-coupling space with a next-to-nearest neighbour coupling. The picture is similar for the adjoint coupling [8].

depend only on $Z(3)$-invariant combinations of Polyakov loops

$$L_j = \mathrm{Tr}\prod_{\tau=1}^{N_\tau} U_0(\mathbf{x}_j,\tau)\,. \tag{2.4}$$

The simplest effective theory is the one with only nearest neighbour interaction terms, whose higher powers can be summed up in closed form to yield [8]

$$Z_{\rm eff} = \int\prod_i dL_i e^{V_i}\prod_{<ij>}(1+2\lambda_1 \mathrm{Re}L_iL_j^*), \quad V_i = \frac{1}{2}\ln(27-18|L_i|^2+8\mathrm{Re}(L_i^3)-|L_i|^4\,. \tag{2.5}$$

The corresponding coupling has been computed to high orders,

$$\lambda(u,N_\tau\geq 5) = u^{N_\tau}\exp\left[N_\tau\left(4u^4+12u^5-14u^6-36u^7+\frac{295}{2}u^8+\frac{1851}{10}u^9+\frac{1055797}{5120}u^{10}+\ldots\right)\right]. \tag{2.6}$$

Note that the next-to-nearest neighbour coupling starts only at $\lambda_2\sim u^{2N_\tau+2}$ while the nearest neighbour coupling of adjoint loops is $\lambda_a\sim u^{2N_\tau}$.

The effective theory is simulated using a standard Metropolis algorithm. Based on the global $Z(3)$ symmetry, one expects spontaneous symmetry breaking for some critical value of the coupling $\lambda_{1,c}$. In Fig. 1 (left) this is signalled by a rise in the Polyakov loop, which on increasing volumes turns into a discontinuous jump corresponding to a first order phase transition. A finite volume scaling analysis indeed provides the correct scaling exponents for a first order transition, and the extrapolation to the thermodynamical limit yield the critical coupling $\lambda_{1c} = 0.187885(30)$.

The influence of the subleading couplings is small as shown in Fig. 1 (right). In a two-coupling theory, there is a critical line separating the ordered and disordered phases. However, not every point on the phase boundary corresponds to a representative of the 4d Yang-Mills theory. These are obtained by the intersections with the lines of fixed N_τ. Since the continuum limit corresponds to $N_\tau\to\infty$, the second coupling quickly becomes negligible as the continuum is approached. We will therefore restrict ourselves to the one-coupling theory for the remainder, for a detailed comparison see [8].

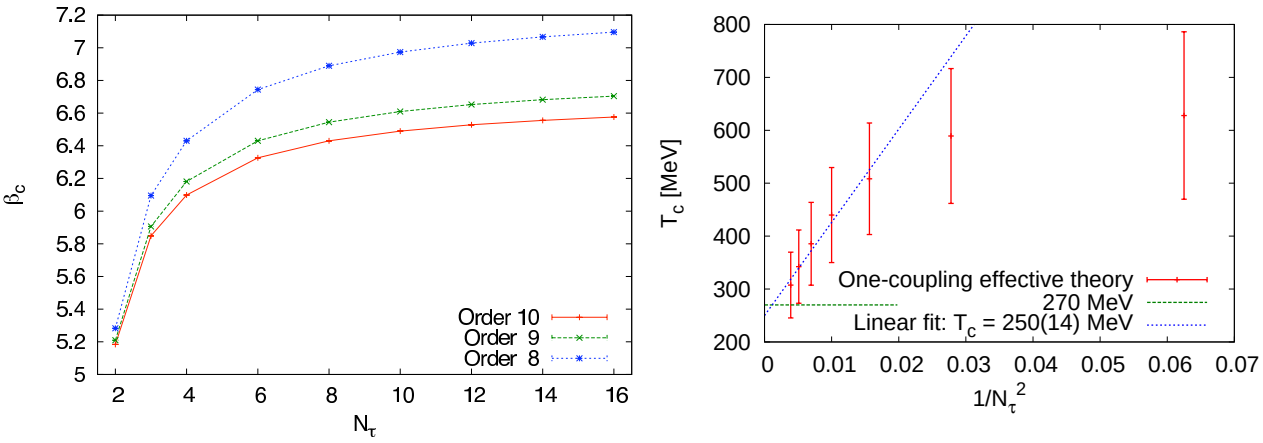

Figure 2: Left: Critical coupling for the $SU(3)$ Yang Mills transition, calculated from $\lambda_{1,c}$ using the maps Eq. (2.6). Right: Critical temperature corresponding to those couplings and continuum extrapolation. Error bars are systematic and denote the difference between the last two orders in the series Eq. (2.6).

With the critical coupling λ_{1c} at hand, the map Eq. (2.6) can be inverted to compute the critical coupling β_c of the 4d Yang-Mills theory for any given N_τ. The result is shown in Fig. 2 (left) for the three highest available truncations of the strong coupling series. The onset of good convergence behaviour is seen. Note that the values for all N_τ are encoded in the map Eq. (2.6) and stem from a single 3d simulation! In [8] a detailed comparison of the values of β_c with those from 4d simulations was made. In the range $N_\tau = 2-16$ the relative error for the predictions of the effective theory was found to be less than 10%. This suggests that a continuum extrapolation may be performed also in the effective theory. Indeed, supplying the Sommer scale r_0 and using the non-perturbative beta-function from [9], the β_c can be converted to critical temperatures and the onset of scaling with leading order additive lattice corrections $\sim a^2 \sim N_\tau^{-2}$ is clearly observed. The continuum extrapolated result $T_c = 250(14)$ MeV is within less than 10% of the full answer from 4d simulations.

3. QCD with very heavy quarks

Let us now summarise the inclusion of heavy fermions [10], which are analytically integrated using the hopping parameter expansion. The quark part of the action for N_f mass-degenerate flavours with masses M is then written as a power series in the hopping parameter κ,

$$-S_q = -N_f \sum_{l=1}^{\infty} \frac{\kappa^l}{l} \mathrm{Tr} H[U]^l, \quad \kappa = \frac{1}{2aM+8}, \quad H[U]_{y,x} = \sum_{\pm\nu} \delta_{y,x+\hat{\nu}} (1+\gamma_\nu), \; \gamma_{-\nu} = -\gamma_\nu \; . \quad (3.1)$$

Thus each hop to a neighbouring lattice site gives a power of the hopping parameter κ . The quark chemical potential μ is introduced as usual by a factor $e^{a\mu}(e^{-a\mu})$ multiplying link variables in positive (negative) time direction. The effective theory is obtained from the full theory in the same way as for Yang-Mills,

$$Z = \int [dU_0][dU_i] \exp[-S_g - S_q] = \int [dU_0] \exp[-S_{\mathrm{eff}}] \; , \quad -S_{\mathrm{eff}} = \ln \int [dU_i] \exp[-S_g - S_q] \; . \quad (3.2)$$

We now have a double expansion in $u(\beta)$ and κ, i.e. all effective couplings depend on both parameters and N_τ. Furthermore, quarks of finite mass lead to terms in the action which explicitly break

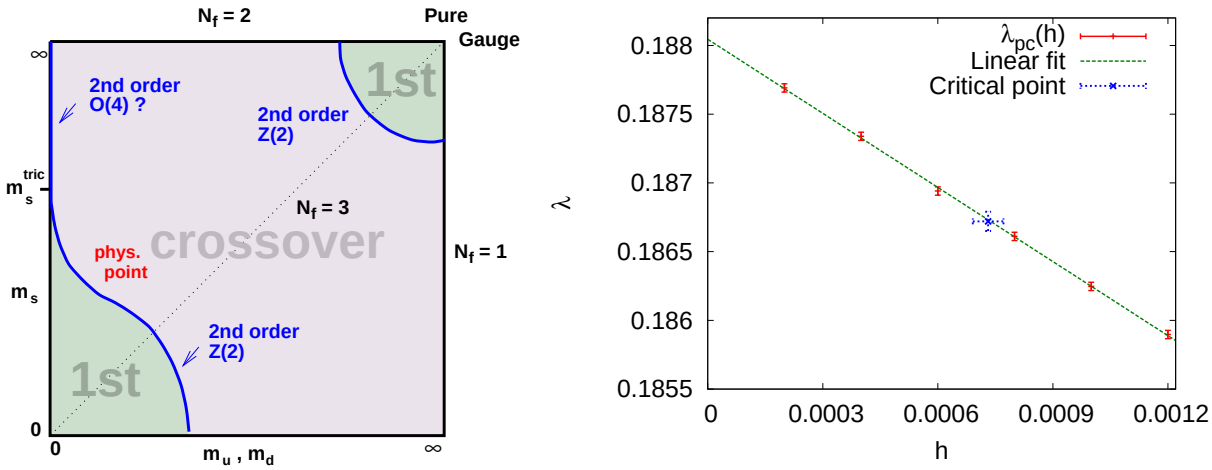

Figure 3: Left: Order of the QCD phase transition as a function of quark masses at $\mu = 0$ (schematic). Right: Calculated phase boundary with critical endpoint.

the $Z(3)$ symmetry present in the pure gauge case. We may arrange this as

$$-S_{\rm eff} = \sum_{i=1}^{\infty} \lambda_i(u,\kappa,N_\tau) S_i^s - 2N_f \sum_{i=1}^{\infty} \left[h_i(u,\kappa,\mu,N_\tau) S_i^a + \bar{h}_i(u,\kappa,\mu,N_\tau) S_i^{a,\dagger} \right] . \tag{3.3}$$

The λ_i are defined as the effective couplings of the $Z(3)$-symmetric terms S_i^s, whereas the h_i multiply the asymmetric terms S_i^a. The h_i and $\bar{h}_i$ are related via $\bar{h}_i(u,\kappa,\mu,N_\tau) = h_i(u,\kappa,-\mu,N_\tau)$.

Keeping the leading fermionic coupling h_1 only and summing up all fermion loops winding multiple times around the torus produces a determinantal expression in the effective theory,

$$Z_{\rm eff} = \int \left(\prod_i dL_i \, e^{V_i} Q_i^{N_f}(h_1,\bar{h_1}) \right) \prod_{<ij>} (1 + 2\lambda_1 {\rm Re} L_i L_j^*) \, . \tag{3.4}$$

with

$$Q_i(h_1,\bar{h_1}) = \left[(1 + h_1 L_i + h_1^2 L_i^* + h_2^3)(1 + \bar{h}_1 L_i^* + \bar{h}_1^2 L_i + \bar{h}_1^3) \right]^2 , \tag{3.5}$$

As a first application we investigate the deconfinement transition of QCD with heavy quarks as a function of quark mass and chemical potential. We begin by considering the case of zero baryon density, shown schematically in Fig. 3 (left). In the pure gauge limit in the upper right corner, the deconfinement transition is of first order. Dynamical quarks at any fixed N_f break the global $Z(3)$ symmetry of the QCD action explicitly. As a consequence, the phase transition weakens with decreasing quark masses until it vanishes at a critical point. For still lighter quarks the deconfinement transition is an analytic crossover. This behaviour is inherited by the effective theory. For a given N_f and $\mu = 0$, we have $h = \bar{h}$ and the effective theory has two couplings, (λ_1, h_1). The first-order phase transition of the one-coupling theory extends to a first-order line with a weakening transition as $h_1$increases. Eventually the transition vanishes at a critical point.

The resulting phase boundary between the ordered and disordered phase is shown in Fig. 3 (right) and found to be linear in the small coupling h_1. In order to locate the critical endpoint we study the scaling of the fourth order Binder cumulant along the phase boundary and find $\lambda_{1c} = 0.18672(7), h_{1c} = 0.000731(40)$. The location of the critical endpoint is marked in Fig. 3 (right).

N_f	M_c/T	$\kappa_c(N_\tau=4)$	$\kappa_c(4)$, Ref. [11]
1	7.22(5)	0.0822(11)	0.0783(4)
2	7.91(5)	0.0691(9)	0.0685(3)
3	8.32(5)	0.0625(9)	0.0595(3)

Table 1: Location of the critical point for $\mu = 0$ and $N_\tau = 4$. The first two columns report our results, the last compares with existing literature.

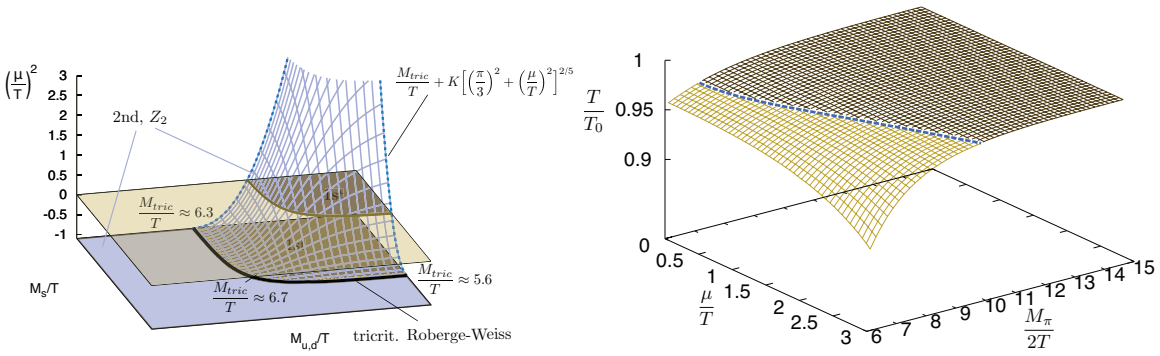

Figure 4: Left: The deconfinement critical surface with heavy quarks. Right: Phase diagram for $N_f = 2$ calculated on $N_\tau = 6$ lattices. Above the surface the theory is deconfined. The line of critical end points (dahsed) separates the crossover (light) from the first order transitions (dark).

As in the case of pure gauge theory, this can be mapped back analytically to predict $\kappa_c(N_\tau)$ for the 4d lattice theory, which can then be compared to full 4d simulations. For $N_\tau = 4$ the results are specified in Table 1, with an accuracy of 5% or better.

With this test passed also for the effective theory with dynamical fermions, it is now easy to switch on chemical potential. In this case $\bar{h}_1 \neq h_1$ and the sign problem enters. However, the sign problem is comparatively mild. Moreover, the effective theory to order κ^2 lends itself to a reformulation in terms of a flux representation as in [6], which is free of the sign problem and can be simulated by a worm algorithm. This allows for a complete determination of the deconfinement transition as a function of quark or pion mass and chemical potential as shown in Fig. 4. The left plot shows the heavy quark (upper right) corner of Fig. 3 (left) extended to real and imaginary chemical potential. The deconfinement critical surface has been computed for all chemical potentials, shown is the result for $N_\tau = 6$ lattices. Note that the μ-dependence of the surface follows the tricritical scaling dictated by the tricritical line at imaginary chemical potential as predicted in [12].

It is now exciting to also apply this effective theory to cold and dense conditions [13]. First, consider the static and strong coupling limits, as in this case the partition function factorises into one-site integrals that can be solved analytically. In the zero temperature limit,

$$Z(\beta=0,\kappa=0) \stackrel{T\to 0}{\longrightarrow} \left[1+4C^{N_c}+C^{2N_c}\right]^{N_s^3} . \tag{3.6}$$

The quark number density is now easily evaluated

$$n = \frac{T}{V}\frac{\partial}{\partial\mu}\ln Z = \frac{1}{a^3}\frac{4N_cC^{N_c}+2N_cC^{2N_c}}{1+4C^{N_c}+C^{2N_c}} , \quad \lim_{T\to 0} a^3 n = \begin{cases} 0, & \mu < m \\ 2N_c, & \mu > m \end{cases} , \tag{3.7}$$

and at zero temperature exhibits a discontinuity when the quark chemical potential equals the mass. Note that this reflects the silver blaze property of QCD, i.e. the fact that the baryon number stays

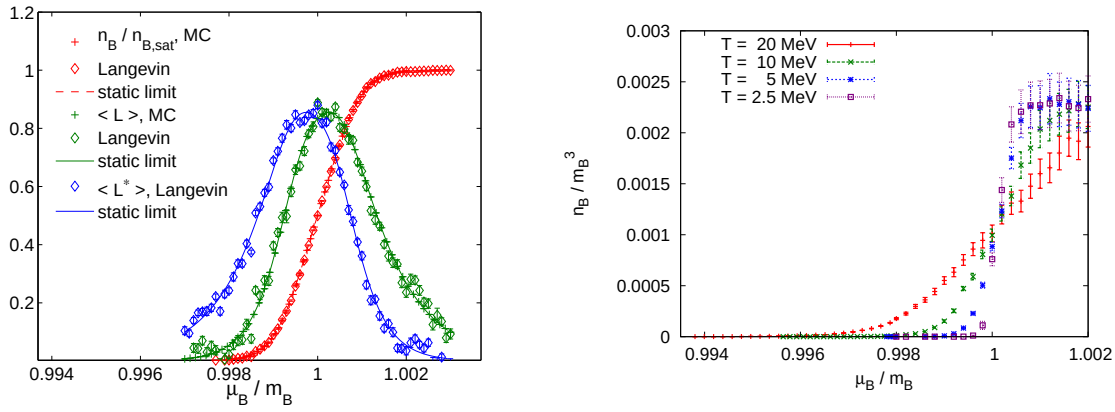

Figure 5: Left: Baryon density, Polyakov loop and conjugate Polyakov loop obtained from Monte Carlo ($N_s = 3$), complex Langevin ($N_s = 6$) and the static strong coupling limit, respectively. Right: Baryon density extrapolated to the continuum. In the zero temperature limit a jump to nuclear matter builds up.

zero for small μ even though the partition function explicitly depends on it. Once the baryon chemical potential is large enough to make a baryon ($m_B = 3M$ in the static strong coupling limit), a transition to the lattice saturation density happens. Note that saturation density here is $2N_c$ quarks per flavour and lattice site and reflects the Pauli priniciple once the lattice is full.

Next, we switch on the gauge coupling as well as the fermionic couplings h_1, h_2 through order κ^2, where the latter also includes $L_i L_j$ terms and hence quark-quark-interaction (for explicit expressions, see [13]). To keep our truncated series in full control, we choose $\beta = 5.7, \kappa = 0.0000887, N_\tau = 116$ corresponding to $m_M = 20$ GeV, $T = 10$ MeV, $a = 0.17$ fm. The effective action has a sign problem and the h_2 term spoils the flux representation used earlier. However, the theory falls into the class of models successfully tested for complex Langevin [14]. Indeed, the corresponding simulation results in Fig. 5 (left) are in complete agreement with those of a Metropolis algorithm, which on small lattices can still be applied up to the onset transition. The silver blaze property as well as lattice saturation are observed also in the interacting case, but the step function is now smoothed. Note that the Polyakov loop as well as its conjugate get screened in the presence of a baryonic medium, and hence rise. The ensuing decrease is due to saturation which forces all $Z(3)$ states to be occupied.

The effective theory being cheap to simulate, we have used up to nine different lattice spacings for all values of chemical potentials, allowing for a continuum extrapolation of the dimensionless ratio n_B/m_B^3, which has leading order $O(a)$ corrections on account of the Wilson fermions. The resulting continuum limit is displayed in Fig. 5 (right) for different temperatures. Again we observe the build-up of a step function as the temperature approaches zero. It is amusing to note that the baryon density at onset, when expressed in units of the baryon mass, is quite similar to the physical nuclear density ≈ 0.16 fm$^{-3} \approx 0.15 \cdot 10^{-2} m^3_{\rm proton}$.

4. Conclusions

We have proposed and tested a treatment of finite density QCD in two steps: an analytic derivation of an effective theory by strong coupling methods, followed by numerical simulations. In the pure gauge sector the effective theory reproduces the correct order of the deconfinement

transition as well as the critical couplings to better than 10% for $SU(2), SU(3)$. When heavy but dynamical quarks are included, the sign problem of the effective theory is mild and can be treated by flux representations or complex Langevin algorithm. The deconfinement transition including its endpoint at finite density has been computed for all chemical potentials. Moreover, the silver blaze property ad the onset of nuclear matter have been seen for the first time directly from QCD.
Acknowledgements: Project supported by the German BMBF, 06MS9150, and by the Helmholtz International Center for FAIR within the LOEWE program launched by the State of Hesse.

References

[1] O. Philipsen, arXiv:1009.4089 [hep-lat].

[2] P. H. Ginsparg, Nucl. Phys. B **170** (1980) 388. T. Appelquist and R. D. Pisarski, Phys. Rev. D **23** (1981) 2305.

[3] K. Kajantie, M. Laine, K. Rummukainen and M. E. Shaposhnikov, Nucl. Phys. B **503** (1997) 357 [hep-ph/9704416].

[4] A. Vuorinen and L. G. Yaffe, Phys. Rev. D **74** (2006) 025011 [hep-ph/0604100]. R. D. Pisarski, Phys. Rev. D **74** (2006) 121703 [hep-ph/0608242].

[5] P. .de Forcrand, A. Kurkela and A. Vuorinen, Phys. Rev. D **77** (2008) 125014 [arXiv:0801.1566 [hep-ph]]. C. Wozar, T. Kaestner, A. Wipf and T. Heinzl, Phys. Rev. D **76** (2007) 085004 [arXiv:0704.2570 [hep-lat]].

[6] C. Gattringer, Nucl. Phys. B **850**, 242 (2011). [arXiv:1104.2503 [hep-lat]].

[7] P. H. Damgaard and H. Hüffel, Phys. Rept. **152**, 227 (1987).

[8] J. Langelage, S. Lottini and O. Philipsen, JHEP **1102** (2011) 057 [Erratum-ibid. **1107** (2011) 014] [arXiv:1010.0951 [hep-lat]].

[9] S. Necco and R. Sommer, Nucl. Phys. B **622** (2002) 328 [hep-lat/0108008].

[10] M. Fromm, J. Langelage, S. Lottini and O. Philipsen, JHEP **1201** (2012) 042 [arXiv:1111.4953 [hep-lat]].

[11] H. Saito *et al.* [WHOT-QCD Collaboration], Phys. Rev. D **84** (2011) 054502 [Erratum-ibid. D **85** (2012) 079902] [arXiv:1106.0974 [hep-lat]].

[12] P. de Forcrand and O. Philipsen, Phys. Rev. Lett. **105** (2010) 152001 [arXiv:1004.3144 [hep-lat]].

[13] M. Fromm, J. Langelage, S. Lottini, M. Neuman and O. Philipsen, arXiv:1207.3005 [hep-lat].

[14] G. Aarts, F. A. James, E. Seiler and I. -O. Stamatescu, Eur. Phys. J. C **71** (2011) 1756 [arXiv:1101.3270 [hep-lat]]. G. Aarts and F. A. James, JHEP **1201** (2012) 118 [arXiv:1112.4655 [hep-lat]].